ISSN 1001-0742
CN 11-2629/X

JES

JOURNAL OF ENVIRONMENTAL SCIENCES

January 1, 2015 Volume 27
www.jesc.ac.cn

Could wastewater analysis be a useful tool for China?

ELSEVIER
Science Press

Sponsored by
Research Center for Eco-Environmental Sciences
Chinese Academy of Sciences

Journal of Environmental Sciences Volume 27 2015

www.jesc.ac.cn

1 The potential risk assessment for different arsenic species in the aquatic environment
Meng Du, Dongbin Wei, Zhuowei Tan, Aiwu Lin, and Yuguo Du

9 Synthesis of linear low-density polyethylene-*g*-poly (acrylic acid)-co-starch/organo-montmorillonite hydrogel composite as an adsorbent for removal of Pb(II) from aqueous solutions
Maryam Irani, Hanafi Ismail, Zulkifli Ahmad, and Maohong Fan

21 Research and application of kapok fiber as an absorbing material: A mini review
Yian Zheng, Jintao Wang, Yongfeng Zhu, and Aiqin Wang

33 Relationship between types of urban forest and $PM_{2.5}$ capture at three growth stages of leaves
Thithanhthao Nguyen, Xinxiao Yu, Zhenming Zhang, Mengmeng Liu, and Xuhui Liu

42 Bioaugmentation of DDT-contaminated soil by dissemination of the catabolic plasmid pDOD
Chunming Gao, Xiangxiang Jin, Jingbei Ren, Hua Fang, and Yunlong Yu

51 Comparison of different combined treatment processes to address the source water with high concentration of natural organic matter during snowmelt period
Pengfei Lin, Xiaojian Zhang, Jun Wang, Yani Zeng, Shuming Liu, and Chao Chen

59 Chemical and optical properties of aerosols and their interrelationship in winter in the megacity Shanghai of China
Tingting Han, Liping Qiao, Min Zhou, Yu Qu, Jianfei Du, Xingang Liu, Shengrong Lou, Changhong Chen, Hongli Wang, Fang Zhang, Qing Yu, and Qiong Wu

70 Could wastewater analysis be a useful tool for China? – A review
Jianfa Gao, Jake O'Brien, Foon Yin Lai, Alexander L.N. van Nuijs, Jun He, Jochen F. Mueller, Jingsha Xu, and Phong K. Thai

80 Controlling cyanobacterial blooms by managing nutrient ratio and limitation in a large hypereutrophic lake: Lake Taihu, China
Jianrong Ma, Boqiang Qin, Pan Wu, Jian Zhou, Cheng Niu, Jianming Deng, and Hailin Niu

87 Reduction of NO by CO using Pd-CeTb and Pd-CeZr catalysts supported on SiO_2 and La_2O_3-Al_2O_3
Victor Ferrer, Dora Finol, Roger Solano, Alexander Moronta, and Miguel Ramos

97 Development and case study of a science-based software platform to support policy making on air quality
Yun Zhu, Yanwen Lao, Carey Jang, Chen-Jen Lin, Jia Xing, Shuxiao Wang, Joshua S. Fu, Shuang Deng, Junping Xie, and Shicheng Long

108 Modulation of the DNA repair system and ATR-p53 mediated apoptosis is relevant for tributyltin-induced genotoxic effects in human hepatoma G2 cells
Bowen Li, Lingbin Sun, Jiali Cai, Chonggang Wang, Mengmeng Wang, Huiling Qiu, and Zhenghong Zuo

115 Impact of dissolved organic matter on the photolysis of the ionizable antibiotic norfloxacin
Chen Liang, Huimin Zhao, Minjie Deng, Xie Quan, Shuo Chen, and Hua Wang

124 Enhanced bio-decolorization of 1-amino-4-bromoanthraquinone-2-sulfonic acid by *Sphingomonas xenophaga* with nutrient amendment
Hong Lu, Xiaofan Guan, Jing Wang, Jiti Zhou, Haikun Zhang

131 Winter survival of microbial contaminants in soil: An *in situ* verification
Antonio Bucci, Vincenzo Allocca, Gino Naclerio, Giovanni Capobianco, Fabio Divino, Francesco Fiorillo, and Fulvio Celico

139 Assessment of potential dermal and inhalation exposure of workers to the insecticide imidacloprid using whole-body dosimetry in China
Lidong Cao, Bo Chen, Li Zheng, Dongwei Wang, Feng Liu, and Qiliang Huang

CONTENTS

147 Biochemical and microbial soil functioning after application of the insecticide imidacloprid
Mariusz Cycoń and Zofia Piotrowska-Seget

159 Comparison of three-dimensional fluorescence analysis methods for predicting formation of trihalomethanes and haloacetic acids
Nicolás M. Peleato and Robert C. Andrews

168 The migration and transformation of dissolved organic matter during the freezing processes of water
Shuang Xue, Yang Wen, Xiujuan Hui, Lina Zhang, Zhaohong Zhang, Jie Wang, and Ying Zhang

179 Genomic analyses of metal resistance genes in three plant growth promoting bacteria of legume plants in Northwest mine tailings, China
Pin Xie, Xiuli Hao, Martin Herzberg, Yantao Luo, Dietrich H. Nies, and Gehong Wei

188 Effect of environmental factors on the complexation of iron and humic acid
Kai Fang, Dongxing Yuan, Lei Zhang, Lifeng Feng, Yaojin Chen, and Yuzhou Wang

197 Resolving the influence of nitrogen abundances on sediment organic matter in macrophyte-dominated lakes, using fluorescence spectroscopy
Xin Yao, Shengrui Wang, Lixin Jiao, Caihong Yan, and Xiangcan Jin

207 Predicting heavy metals' adsorption edges and adsorption isotherms on MnO_2 with the parameters determined from Langmuir kinetics
Qinghai Hu, Zhongjin Xiao, Xinmei Xiong, Gongming Zhou, and Xiaohong Guan

217 Applying a new method for direct collection, volume quantification and determination of N_2 emission from water
Xinhong Liu, Yan Gao, Honglian Wang, Junyao Guo, and Shaohua Yan

225 Effects of water management on arsenic and cadmium speciation and accumulation in an upland rice cultivar
Pengjie Hu, Younan Ouyang, Longhua Wu, Libo Shen, Yongming Luo, and Peter Christie

232 Acid-assisted hydrothermal synthesis of nanocrystalline TiO_2 from titanate nanotubes: Influence of acids on the photodegradation of gaseous toluene
Kunyang Chen, Lizhong Zhu, and Kun Yang

241 Air-soil exchange of organochlorine pesticides in a sealed chamber
Bing Yang, Baolu Han, Nandong Xue, Lingli Zhou, and Fasheng Li

251 Effects of elevated CO_2 on dynamics of microcystin-producing and non-microcystin-producing strains during *Microcystis* blooms
Li Yu, Fanxiang Kong, Xiaoli Shi, Zhen Yang, Min Zhang, and Yang Yu

259 Sulfide elimination by intermittent nitrate dosing in sewer sediments
Yanchen Liu, Chen Wu, Xiaohong Zhou, David Z. Zhu, and Hanchang Shi

266 Steel slag carbonation in a flow-through reactor system: The role of fluid-flux
Eleanor J. Berryman, Anthony E. Williams-Jones, and Artashes A. Migdisov

276 Amine reclaiming technologies in post-combustion carbon dioxide capture
Tielin Wang, Jon Hovland, and Klaus J. Jens

290 Do vehicular emissions dominate the source of C6-C8 aromatics in the megacity Shanghai of eastern China?
Hongli Wang, Qian Wang, Jianmin Chen, Changhong Chen, Cheng Huang, Liping Qiao, Shengrong Lou, and Jun Lu

298 Insights into metals in individual fine particles from municipal solid waste using synchrotron radiation-based micro-analytical techniques
Yumin Zhu, Hua Zhang, Liming Shao, and Pinjing He

Available online at www.sciencedirect.com

ScienceDirect

www.journals.elsevier.com/journal-of-environmental-sciences

JOURNAL OF ENVIRONMENTAL SCIENCES

www.jesc.ac.cn

Chemical and optical properties of aerosols and their interrelationship in winter in the megacity Shanghai of China

Tingting Han[1], *Liping Qiao*[2], *Min Zhou*[2], *Yu Qu*[3], *Jianfei Du*[4], *Xingang Liu*[1,*], *Shengrong Lou*[2], *Changhong Chen*[2], *Hongli Wang*[2,*], *Fang Zhang*[5], *Qing Yu*[1], *Qiong Wu*[1]

1. *State Key Laboratory of Water Environment Simulation, School of Environment, Beijing Normal University, Beijing 100875, China*
2. *State Environmental Protection Key Laboratory of Cause and Prevention of Urban Air Pollution Complex, Shanghai Academy of Environmental Sciences, Shanghai 200233, China*
3. *State Key Laboratory of Atmospheric Boundary Layer Physics and Atmospheric Chemistry, Institute of Atmospheric Physics, Chinese Academy of Sciences, Beijing 100029, China*
4. *Shanghai Meteorological Service, Shanghai 200000, China*
5. *College of Global Change and Earth System Science, Beijing Normal University, Beijing 100875, China*

ARTICLE INFO

Article history:
Received 19 February 2014
Revised 7 April 2014
Accepted 11 April 2014
Available online 24 November 2014

Keywords:
Optical properties
Diurnal variations
Chemical apportionment
Shanghai

ABSTRACT

A field campaign on air quality was carried out in Shanghai in winter of 2012. The concentrations of NO, NO_2, NOx, SO_2, CO, and $PM_{2.5}$ increased during haze formation. The average masses of SO_4^{2-}, NO_3^- and NH_4^+ were 10.3, 11.7 and 6.7 μg/m^3 during the haze episodes, which exceeded the average (9.2, 7.9, and 3.4 μg/m^3) of these components in the non-haze days. The mean values for the aerosol scattering coefficient (b_{sp}), aerosol absorption coefficient (b_{ap}) and single scattering albedo (SSA) were 288.7, 27.7 and 0.91 Mm^{-1}, respectively. A bi-peak distribution was observed for the mass concentrations of CO, NO, NO_2, and NOx. More sulfate was produced during daytime than that in the evening due to photochemical reactions. The mass concentration of NH_4^+ achieved a small peak at noontime. NO_3^- showed lower concentrations in the afternoon and higher concentrations in the early morning. There were obvious bi-peak diurnal patterns for b_{sp} and b_{ap} as well as SSA. b_{sp} and b_{ap} showed a positive correlation with $PM_{2.5}$ mass concentration. $(NH_4)_2SO_4$, NH_4NO_3, organic mass, elemental carbon and coarse mass accounted for 21.7%, 19.3%, 31.0%, 9.3% and 12.3% of the total extinction coefficient during non-haze days, and 25.6%, 24.3%, 30.1%, 8.1% and 8.2% during hazy days. Organic matter was the largest contributor to light extinction. The contribution proportions of ammonium sulfate and ammonium nitrate to light extinction were significantly higher during the hazy time than during the non-haze days.

© 2014 The Research Center for Eco-Environmental Sciences, Chinese Academy of Sciences. Published by Elsevier B.V.

* *Corresponding authors*. E-mails: liuxingang@bnu.edu.cn (Xingang Liu), wanghl@saes.sh.cn (Hongli Wang).

http://dx.doi.org/10.1016/j.jes.2014.04.018
1001-0742/© 2014 The Research Center for Eco-Environmental Sciences, Chinese Academy of Sciences. Published by Elsevier B.V.

jesc.ac.cn

Introduction

Aerosols, consisting of liquid and solid particles suspended in the air, are important components in the atmosphere. Airborne aerosols play a significant role in visibility (Watson, 2002; Liu et al., 2013a), regional air quality (Han et al., 2014a,2014b,2014c; Liu et al., 2013b), and climate change (Liu et al., 2012). Chemical components in the aerosols, such as sulfate, nitrate, ammonium, black carbon (BC), particulate organic matter (POM), and other chemical species, can scatter and absorb the incident light and therefore lead to atmospheric dimming and horizontal visibility degradation (Liu et al., 2008; Jung et al., 2009). Several key aerosol optical properties (AOPs), including the atmospheric aerosol burden, single scattering albedo (ω), upscatter fraction and the mass scattering and absorption efficiencies, must be measured or estimated in order to evaluate the local or regional climate effect of aerosols (Chýlek and Wong 1995; Liu et al., 2012). To fully understand the aerosol optical properties, extensive sets of both in situ and remote measurements are required (Alados-Arboledas et al., 2008). Consequently, several observation networks of aerosol optical properties have been established internationally to observe aerosol optical characterization such as AERONET (AErosol RObotic NETwork), SKYNET (SKY Network), AEROCAN (Canadian Sunphotometer Network), RIMA (Red Ibérica de Medida de Aerosoles), AGSNet (Aerosol Ground Station Network) and so on (Holben et al., 1998; Goloub et al., 2008; Uchiyama et al., 2005; Bokoye et al., 2001; Campanelli et al., 2007; O'Brien and Mitchell, 2003).

Along with rapid economic growth and urbanization, the megacities in China are experiencing severe air pollution problems (Chan and Yao, 2008; Liu et al., 2013b; Han et al., 2014c). The annual average of PM_{10} (particulate matter with diameter smaller than 10 μm) concentrations in 113 key cities in China was 82 $\mu g/m^3$, which is about 4–6 times that in the developed countries (Wang and Hao, 2012). Visibility degradation caused by enhanced aerosol concentrations has become a pervasive phenomenon in the regions with dense population and fast industrialization (Wang et al., 2009; Liu et al., 2013b). Sulfate, nitrate, ammonium, POM, and BC have been identified as the major chemical components in fine particles in Chinese megacities and contribute over 90% of the extinction coefficient (Cao et al., 2012; Wang et al., 2012; Zhang et al., 2012a; Han et al., 2014a,2014b,2014c). In addition, previous studies showed that sulfate and organic mass are the main chemical components contributing to the light extinction and visibility degradation (Cheung et al., 2005; Yang et al., 2007; Tao et al., 2009; Liu et al., 2012). Huang et al. (2012a) investigated the proportion of chemical components in $PM_{1.0}$ in Shanghai during 15 May to 10 June 2010 and reported that sulfate was the most abundant component (on average accounting for 33.3% of the total mass) followed by OM (28.7%), nitrate (16.3%), ammonium (13.4%), BC (6.7%), and chloride (1.6%). Many articles have been dedicated to aerosol optical properties and their variation measured at worldwide locations (Bergin et al., 2001; Formenti et al., 2002; Andreae et al., 2008; Jung et al., 2009; Lyamani et al., 2008; Liu et al., 2013b). Chan et al. (1999) calculated the contribution of chemical species to aerosol scattering and absorption. Liu et al. (2009) focused on particle hygroscopic influences on aerosol scattering and absorbing processes. There have been many papers focused on the characteristics of chemical compositions or the optical properties of aerosol alone, while papers about the relationship between chemical compositions and optical properties of aerosol are very limited in China. Thus, it is necessary to study the characteristics of aerosol optical properties and the associated chemical apportionments to understand the causes of visibility degradation.

In this article, we described the characteristics of gaseous pollutants and water-soluble inorganic ions, and then analyzed their diurnal variation. Secondly, we presented intensive measurements of aerosol optical properties such as aerosol scattering and absorption coefficients and SSA (single scattering albedo) in downtown Shanghai, and then analyzed their diurnal variation. Finally, the correlation between aerosol optical parameters and chemical compositions was investigated.

1. Experiment

1.1. Experimental site

Shanghai, with a population of over 20 million, is the largest commercial and industrial city in China, as well as a famous mega-city in the world. The gross domestic product (GDP) in 2012 exceeded 312 billion U.S. dollars with an annual growth rate of 7.5% (http://www.stats-sh.gov.cn/). Furthermore, the total energy consumption was 112.7 million tons of coal equivalents (TCE) by the end of 2011. Shanghai had about 3.3 million cars, with an annual increase of 6.3%. (http://www.stats-sh.gov.cn/data/toTjnj.xhtml?y=2012). High degrees of industrial and metropolitan emissions had unavoidably resulted in heavy emission of air pollutants in Shanghai. Field measurements in an urban site of Shanghai were carried out from December 1 to 31, 2012 in the yard of Shanghai Academy of Environmental Sciences (31.17°N, 121.43°E), which is located in the southwest of urban Shanghai and is about 8 km away from the city center. The sample inlet was on the roof of a 5-floor building (~15 m above the ground). There were no buildings blocking observations at this height and the air mass could smoothly flow through the area.

1.2. Instrumentation and measurements

Instruments used in this study are listed in Table 1. Mass concentrations of PM_{10} and $PM_{2.5}$ were measured by particulate monitors (Thermo, FH62C-14). Water-soluble ionic components (WSIC) such as NH_4^+, NO_3^- and SO_4^{2-} in $PM_{2.5}$ were measured by MARGA (Monitor for AeRosols and GAses in Ambient Air). Gaseous pollutants (SO_2, NO–NO_2–NOx, O_3, CO) were detected by an SO_2 Analyzer (Ecotech, EC9580B), NO–NO_2–NOx Analyzer (Thermo scientific 42i), O_3 Analyzer (Ecotech, EC9810B) and CO Analyzer (Ecotech, EC9830B), respectively. The aerosol scattering coefficient at dry conditions b_{sp} and aerosol absorption coefficient b_{ap} were measured by an Integrating Nephelometer (Aurora 3000) and Aethalometer (Magee AE31), respectively. It should be noted that the wavelengths of b_{sp} and b_{ap} were different, thus, b_{sp} and b_{ap} values at different wavelengths were fitted by a power-law equation and then b_{sp} and b_{ap} values at 550 nm could be calculated (Liu et al., 2012). In addition, atmospheric visibility was measured by a visibility sensor (Belfort Model 6000). Elemental carbon (EC) and organic carbon (OC) were monitored by a semi-continuous OC/EC analyzer (RT-4 model, Sunset Laboratory Inc.) equipped with a $PM_{2.5}$ cyclone and an upstream parallel-plate organic denuder (Sunset Laboratory Inc.). Meteorological parameters including RH (relative humidity) were monitored by an automatic meteorological station (Metone). All of the instruments mentioned above were calibrated according to their manufacturers' manuals.

jesc.ac.cn

Table 1 – Overview of instruments involved in this study.

Instrument	Parameter	Manufacturer model	Calibration	Resolution	Wavelength (nm)
Particulate monitor	$PM_{1.0}/PM_{2.5}/PM_{10}$	Thermo FH 62C-14	Zero, span check every month	5 min	/
SO_2 analyzer	SO_2	Ecotech EC9580B	Zero, span check every two weeks	5 min	/
NO–NO_2–NOx analyzer	NO–NO_2–NOx	Thermo scientific 42i	Zero, span check every two weeks	5 min	/
O_3 analyzer	O_3	Ecotech EC9810B	Zero, span check every two weeks	5 min	/
CO analyzer	CO	Ecotech EC9830B	Zero, span check every two weeks	5 min	/
RH sensor	RH	Metone	/	1 min	/
Visibility sensor	Visibility	Belfort Model 6000	Zero, span check every six months	1 min	
Integrating nephelometer	Aerosol scattering coefficient	Aurora3000	Zero check every day; Span check every week by CO_2	5 min	450/525/635
MARGA	NH_4^+, NO_3^- and SO_4^{2-}	ADI 2080	IC calibration before and after the campaign	30 min	/
Semi-continuous OC/EC analyzer	OC/EC mass concentration	Sunset. RT4	Zero, span check every two weeks	1 hr	/
Aethalometer	Black carbon	Magee AE31	Zero check every week	5 min	370/470/520/590/660/880/950

The light extinction coefficient, b_{ext}, which is wavelength dependent, can be expressed by Eq. (1) as the sum of scattering (b_{scat}) and absorption (b_{abs}) by gases and particles.

$$b_{ext} = b_{scat} + b_{abs} = b_{sg} + b_{sp} + b_{ag} + b_{ap} \quad (1)$$

where, b_{scat} is the sum of scattering by gases b_{sg} and particles b_{sp}, and b_{abs} is the sum of absorption by gases b_{ag} and particles b_{ap}. b_{sg} is referred to as Rayleigh scattering (10 Mm^{-1} at ground level), and b_{sp}, which is the largest contributor to total light extinction in most areas (Chan et al., 1999; Liu et al., 2013b), is caused by both fine and coarse particles. b_{ag} is mainly due to absorption of nitrogen dioxide (NO_2), while b_{ap} is primarily caused by EC particles.

The approach used in the IMPROVE (The Interagency Monitoring of Protected Visual Environments) program to estimate light extinction for aerosol components assumes externally mixed aerosols. The reconstructed b_{ext} can then be calculated from the mass concentrations of the aerosol components by Eq. (2), based on the original IMPROVE algorithm (Malm and Hand, 2007).

$$b_{ext} = 3f(RH) \times [(NH_4)_2SO_4] + 3f(RH) \times [NH_4NO_3] + 4 \times [POM] + 10 \times [EC] + 1 \times [FineSoil] + 0.6 \times [Coarses] + 0.161 \times [NO_2] + 10 \quad (2)$$

$$[(NH_4)_2SO_4] = 0.944 \times [NH_4^+] + 1.02 \times [SO_4^{2-}] \quad (3)$$

$$[NH_4NO_3] = 1.29 \times [NO_3^-] \quad (4)$$

$$[POM] = 1.6 \times [OC] \quad (5)$$

$$[FineSoil] = 2.49 \times [Si] + 2.2 \times [Al] + 2.42 \times [Fe] + 1.63 \times [Ca] + 1.94 \times [Ti] \quad (6)$$

$$[CoarseMass] = PM_{10} - PM_{2.5} \quad (7)$$

Eq. (2) includes a constant 10 Mm^{-1}, which denotes the Rayleigh scattering of clear air (Malm and Hand, 2007). The light extinction coefficients of atmospheric aerosol are expressed in

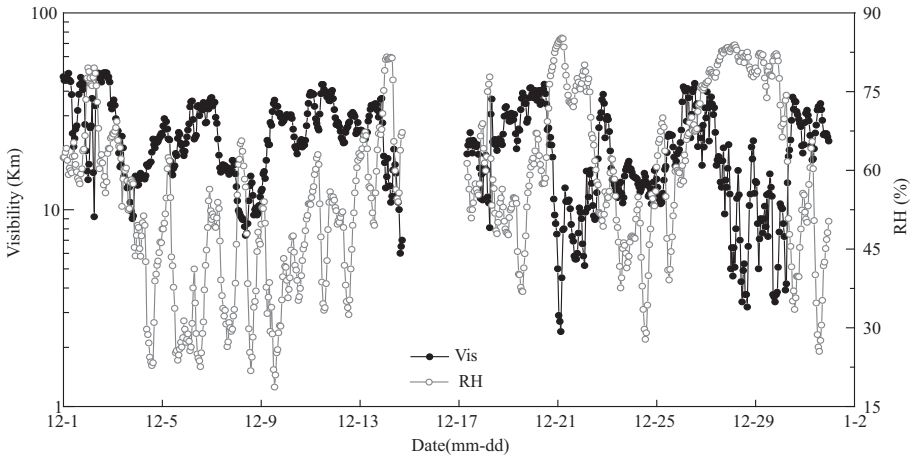

Fig. 1 – Time series of visibility and relative humidity (RH) in Shanghai during the whole campaign.

jesc.ac.cn

Mm^{-1}. The chemical composition concentrations shown in brackets are in units of $\mu g/m^3$. Dry efficiency terms are in units of m^2/g; and the hygroscopic growth terms, f(RH), are unitless. EC is referred to as light-absorbing carbon (b_{ap} = 10[EC]), and the mass extinction coefficient of hygroscopic aerosol implies a RH-dependent scaling factor (f(RH)), which represents the relationship between RH and the scattering efficiency. Eqs. (3) and (4) assume that SO_4^{2-} and NO_3^- are fully neutralized by NH_4^+.

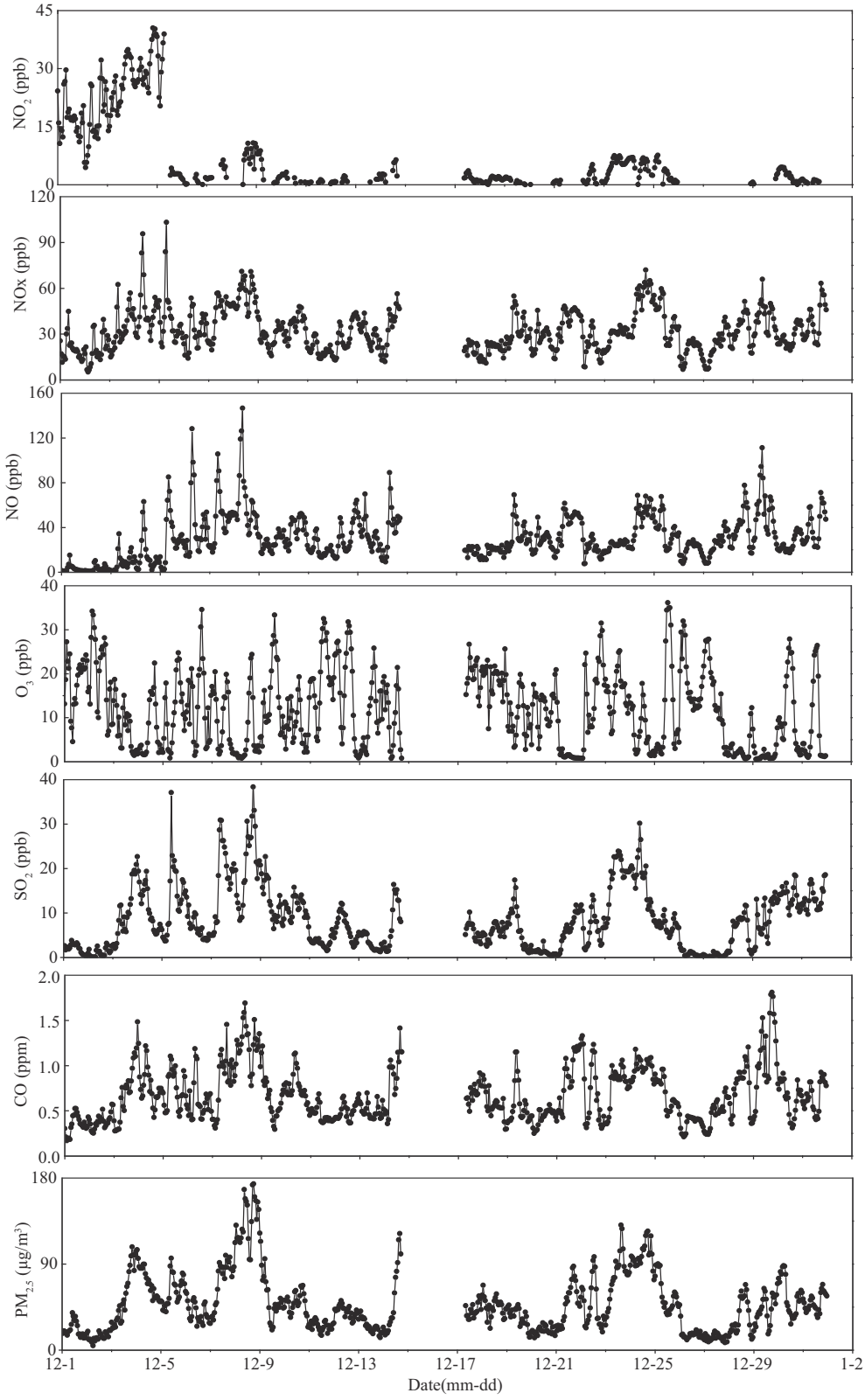

Fig. 2 – Time series of observed NO_2, NOx, NO, O_3, SO_2, CO, and $PM_{2.5}$ in Shanghai during 1–31 December, 2012.

jesc.ac.cn

POM was estimated by multiplying the measured OC by a factor (1.6) to compensate for other atoms such as H, O and N in the organic molecules (Turpin and Lim, 2001).

2. Results and discussion

2.1. Process of haze

2.1.1. Temporal variations of gaseous pollutants and aerosol chemical compositions

Temporal distributions of visibility and RH in Shanghai are illustrated in Fig. 1. The relationship between visibility and RH is a negative correlation, that is, the visibility reaches the minimum value of the day in the middle of the night while RH reaches the maximum, and vice versa. According to the definition of haze (visibility < l0 km and RH < 90%) (Wu et al., 2006), there were seven haze episodes observed in Shanghai in the time periods of December 8 2:00–11:00, December 8 17:00–21:00, December 20 21:00–06:00, December 21 13:00–03:00, December 28 0:00–17:00, December 29 02:00–12:00 and December 29 17:00–06:00, and the other days during the campaign could be classified as non-haze days. The hazy time accounted for 11.4% of the whole campaign. Temporal variations of the measured NO_2, NOx, NO, O_3, SO_2, CO, and $PM_{2.5}$ from 1–31 December 2012 are depicted in Fig. 2. Generally, the concentrations of air pollutants NO_2, NOx, NO, SO_2, CO, and $PM_{2.5}$ had an increasing trend during the haze episodes. The pollutants SO_2, NO_2 and CO, being the emissions from fuel and coal burning, had the same increasing trend from 1–9 December, with maximum instantaneous values of 38.4, 40.5 ppb and 1.8 ppm, respectively. The mass loading of $PM_{2.5}$ gradually accumulated, and its instantaneous value reached 173.8 μg/m^3 at LST 18:00 of 8 December with an averaged value of 75.5 μg/m^3 during the haze episode, which was nearly two times as high as the daily limit (35 μg/m^3) of the USA Ambient Air Quality Standard. O_3, which is formed by photochemical reactions between volatile organic compounds (VOCs) and nitrogen oxides (NOx) in the presence of heat and sunlight (Seinfeld and Pandis, 2006), showed a cyclical variation and reached a maximum value at noon.

Time series of the mass concentrations of SO_4^{2-}, NO_3^- and NH_4^+ are shown in Fig. 3. The average values of SO_4^{2-}, NO_3^- and NH_4^+ were 10.3, 11.7 and 6.7 μg/m^3 during the haze episodes in Shanghai, which all exceeded the averages (9.2, 7.9, and 3.4 μg/m^3) of these components during the non-haze days (Table 2). Du et al. (2011) reported the corresponding values of SO_4^{2-} (28.7 μg/m^3), NO_3^- (32.9 μg/m^3) and NH_4^+ (19.3 μg/m^3) during the haze events in Shanghai from May 27 to June 16, 2009. The results of this study are also smaller than those reported from urban Beijing (49.8, 31.4 and 25.8 μg/m^3) from August 18 to September 8, 2006 on the campus of Peking University (Han et al., 2004c).

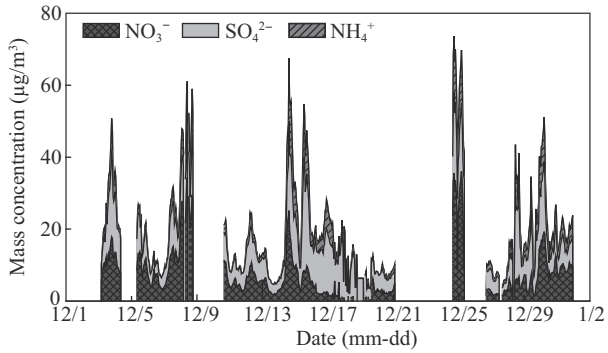

Fig. 3 – Time series of NO_3^-, SO_4^{2-} and NH_4^+ mass concentrations in Shanghai during 1–31 December, 2012.

2.1.2. Temporal variations of atmospheric optical properties

Temporal variations of the optical properties of aerosols in Shanghai from December 1 to 31 are depicted in Fig. 4. The atmospheric aerosol scattering coefficient b_{sp}, aerosol absorption coefficient b_{ap}, and single scattering albedo ω at 550 nm during the whole campaign in Shanghai were 288.7 (186.3), 27.7 (17.6) and 0.91 (0.04) Mm^{-1}, expressed as mean and standard deviation (S.D.), respectively. Generally, aerosol optical parameters in this study were lower in magnitude than those at other sites in China. Li et al. (2007) reported b_{sp} = 468 ± 472 Mm^{-1} and b_{ap} = 65 ± 75 Mm^{-1} in March 2005 at the rural site Xianghe (~70 km southeast of Beijing). The results of this study are also smaller than those reported at urban Guangzhou ($b_{sp,545}$ = 463 ± 178 and $b_{ap,532}$ = 92 ± 62 Mm^{-1}) (Andreae et al., 2008), but are similar to those from a study in Shanghai ($b_{sp,532}$ = 293 ± 206 and $b_{ap,532}$ = 66 ± 47Mm^{-1}) from 1 December 2010 to 31 March 2011 (Xu et al., 2012).

The single scattering albedo, ω_λ, is the ratio of the scattering coefficient over the extinction coefficient at a given wavelength. Here, ω has been calculated at λ = 550 nm by Eq. (8).

$$\omega_{550} = \frac{bsp}{bsp + bap} \quad (8)$$

The single scattering albedo reflects the scattering power of the atmospheric particulate matter. Mean SSA was 0.91 during the experimental period, which indicated a higher proportion of scattering particulate matter at the urban site, similar to the values of 0.93 in Lin'an (Xu et al., 2002) and 0.88 in Gosan (Kim et al., 2004), but remarkably larger than 0.68 at the Pedregal site of Mexico City (Eidels-Dubovoi, 2002).

2.2. Diurnal variations

2.2.1. Diurnal variations of gaseous pollutants and aerosol chemical compositions

Fig. 5 presents the diurnal variations of different species during the campaign. The major source of O_3 is photochemical reactions, and the concentrations of O_3 are closely connected with the solar radiation intensity (Seinfeld and Pandis, 2006). At night, the O_3 concentration in the atmosphere remained almost at zero, and the O_3 concentration began to rise slowly with the strengthening of solar radiation after sunrise. At 13:00 LST the concentration of O_3 reached the peak of the day. Subsequently, the O_3 concentration showed a slow downward trend. A bi-peak distribution was observed for the mass concentrations of CO, NO_2, NOx and NO as shown in Fig. 5. For all of these four species, the two peaks appeared at morning (7:00–8:00 LST) and nightfall (17:00–18:00 LST), respectively. The emergence of the two peaks was mainly attributed to the combustion of fossil fuels during

jesc.ac.cn

Table 2 – Statistical summary of chemical species, visibility and RH during the non-haze days and haze days in Shanghai.

Index	Start time	Duration (hour)	Visibility (km)	RH (%)	$PM_{2.5}$ ($\mu g/m^3$)	NO_3^- ($\mu g/m^3$)	SO_4^{2-} ($\mu g/m^3$)	NH_4^+ ($\mu g/m^3$)	NO (ppb)	NO_x (ppb)	SO_2 (ppb)	CO (ppm)	O_3 (ppb)
Haze days	2012-12-8 02:00	10	8.7	57.9	131.2	28.0	12.7	9.1	86.2	58.2	14.9	1.4	2.4
	2012-12-8 17:00	5	9.7	39.7	160.0	28.5	15.5	11.8	54.3	62.2	28.0	1.3	3.0
	2012-12-20 21:00	10	5.9	84.2	22.2	3.4	4.4	1.2	22.1	22.4	1.1	0.5	10.3
	2012-12-21 13:00	15	7.3	76	64.2	/	/	/	47.5	41.7	9.0	1.1	1.1
	2012-12-28 00:00	18	6.5	82.3	37.5	4.7	13.0	4.9	40.9	33.7	6.8	0.8	2.0
	2012-12-29 02:00	11	8.4	79.6	44.9	4.5	11.3	4.5	68.1	45.4	7.4	1.1	1.1
	2012-12-29 17:00	14	6.1	75.7	68.5	13.0	15.5	8.4	34.1	32.9	13.4	1.2	4.6
Average			7.5	70.8	75.5	11.7	10.3	6.7	50.5	42.4	11.5	1.1	3.5
Non-haze days			22.2	56.4	49.1	7.9	9.2	3.4	19.9	32.2	8.7	0.7	11.7

the morning and evening traffic rush hours. After the morning rush hour, the CO, NO_2, NOx and NO concentrations showed slow downward trends, which probably was the result of strong atmospheric mixing and dilution due to the elevated height of the atmospheric planetary boundary layer (PBL). After sunset (18:00 LST), the formation of a stable nocturnal PBL in atmospheric inversion led to a low atmospheric diffusion ability, and thus resulted in high concentrations throughout the night. The diurnal variations of CO, NO_2, NOx and NO were very similar, which indicated that these gaseous pollutants may come from the same sources. The concentration of SO_2 reached a maximum at 9:00 LST and then maintained at a relatively constant level.

The diurnal variations of SNA (sulfate, nitrate, and ammonium) are presented in Fig. 6. Following the increasing solar radiation during daytime, the photochemistry was more active and therefore produced more sulfate during daytime than in the evening. The diurnal variation of sulfate showed two peaks at 15:00 LST. The mass concentration of ammonium kept at a lower level before 12:00 LST, then achieved a small peak at 12:00 LST. The time when it reached the second peak was 17:00 LST, and the maximum of daily-averaged mass concentration of NH_4^+ was 4.5 $\mu g/m^3$. As shown in Fig. 6c, nitrate showed little hourly variation, indicating that it was well mixed in the boundary layer. In addition, the nitrate showed lower concentrations in the afternoon and higher concentrations in the early morning, suggesting that boundary layer variation and gas–aerosol partitioning were the dominant control mechanisms for its diurnal patterns (Huang et al., 2012a,2012b).

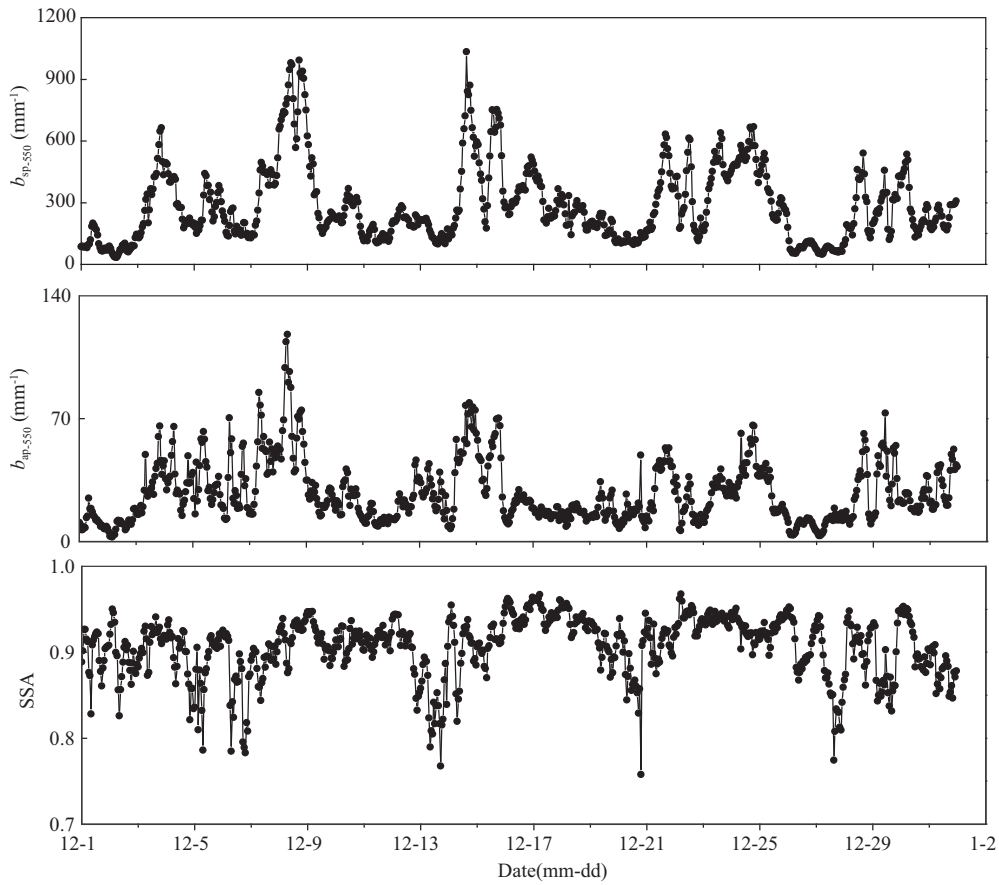

Fig. 4 – Time series of the measured aerosol scattering coefficient b_{sp}, aerosol absorption coefficient b_{ap}, and single scattering albedo (SSA) in Shanghai during 1–31 December, 2012.

jesc.ac.cn

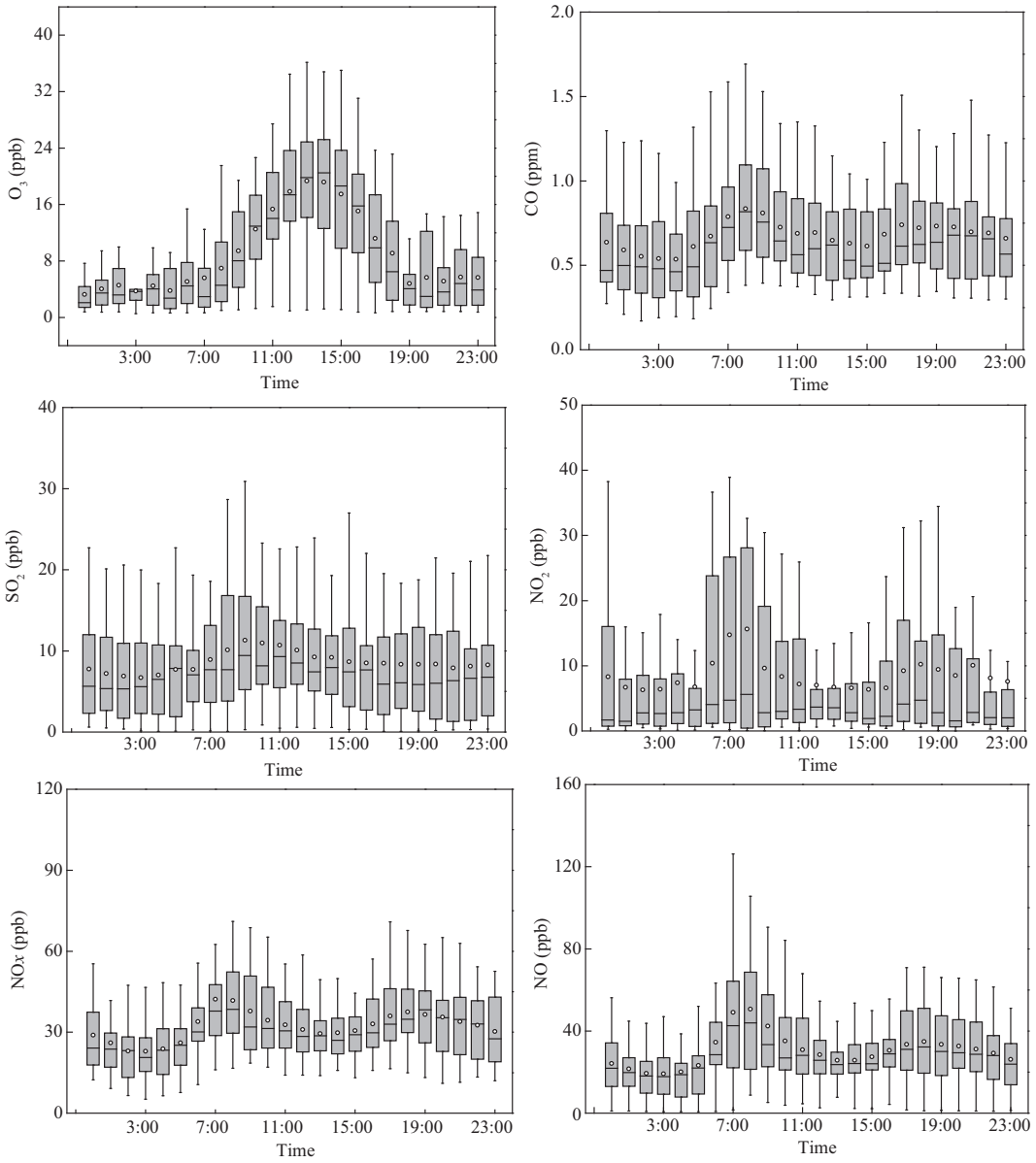

Fig. 5 – Diurnal variations of O_3; CO; SO_2; NO_2; NOx and NO in Shanghai. The dot is the mean value, the horizontal line in the box is the median, the limits of the boxes are the 25th percentile and 75th percentile, and the vertical lines extend to 5th and 95th percentiles for each 1-hr period after the indicated start time.

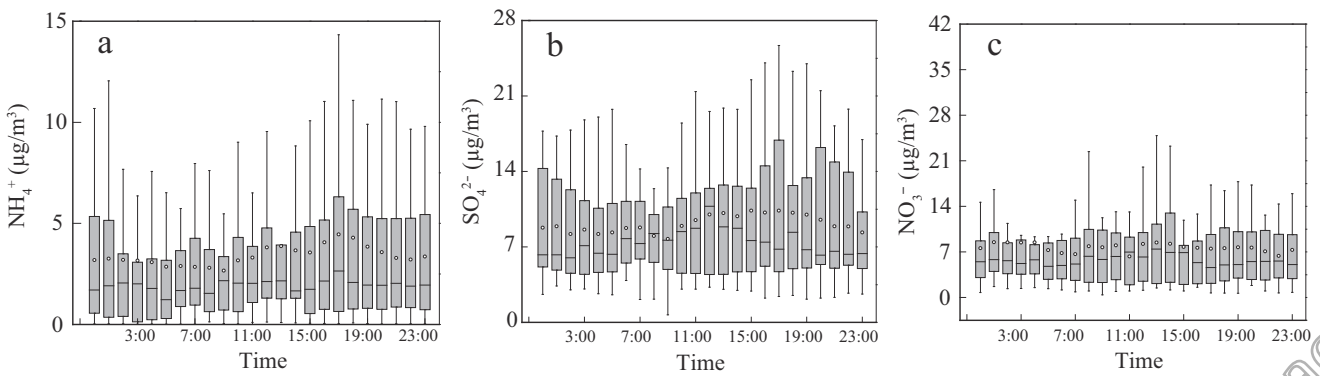

Fig. 6 – Diurnal variations of (a) NH_4^+, (b) SO_4^{2-}, and (c) NO_3^- mass concentrations in Shanghai. Symbols are analogous to Fig. 5.

jesc.ac.cn

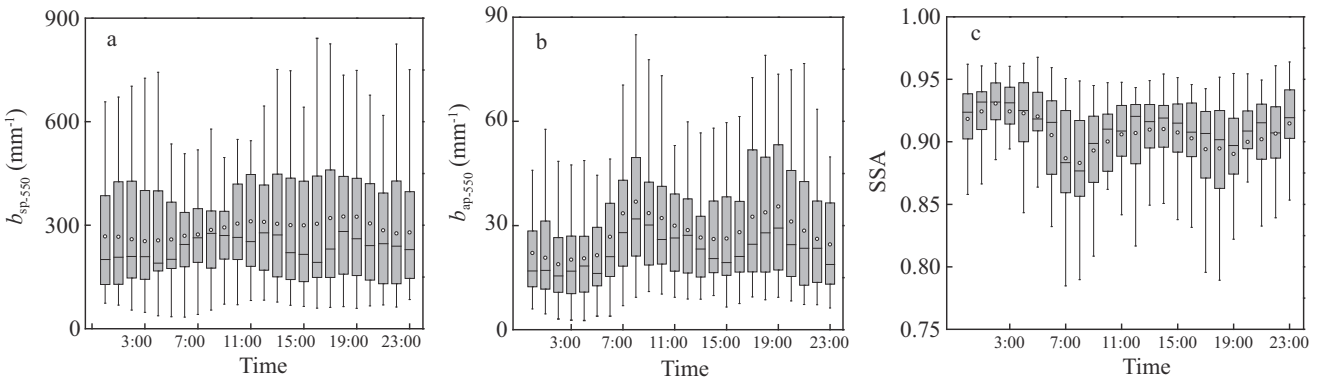

Fig. 7 – Diurnal variations of (a) b_{sp}; (b) b_{ap} and (c) SSA (single scattering albedo) in Shanghai. Symbols are analogous to Fig. 5.

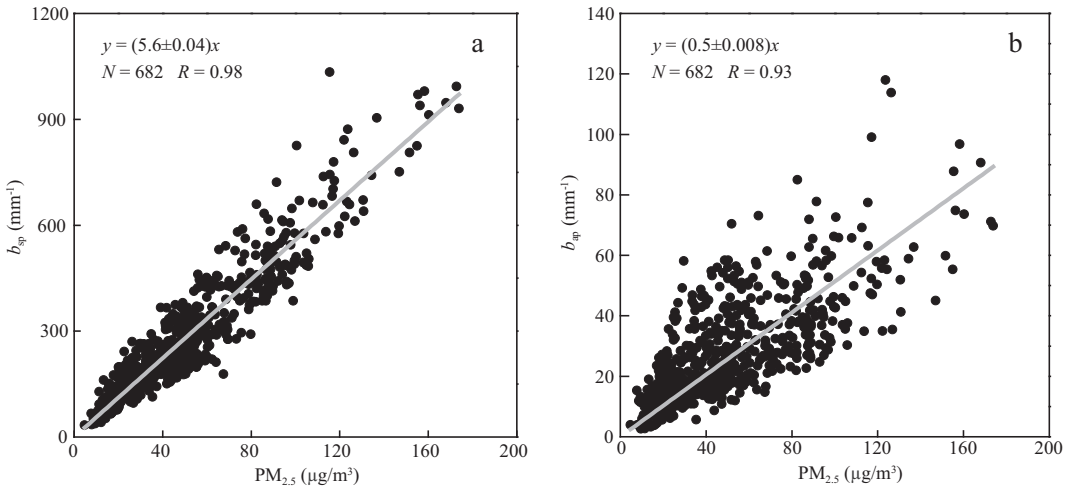

Fig. 8 – Relationship between the mass concentration of $PM_{2.5}$ and (a) b_{sp}; (b) b_{ap} in Shanghai.

2.2.2. Diurnal variations of atmospheric optical properties

Fig. 7 shows diurnal variation of b_{sp} and b_{ap} as well as SSA based on hourly averages. There were obvious bi-peak diurnal patterns for all variables. As is clear in Fig. 7, the diurnal variation of b_{sp} showed two peaks, which occurred at 11:00 LST and 18:00 LST. For b_{sp}, peak values were 310.9 and 324.6 Mm^{-1}. The scattering coefficient b_{sp} showed a decrease between 11:00 LST and 15:00 LST, which might be due to the increase of the height of the PBL. Fig. 7b displays the diurnal cycle for b_{ap}, which was even more pronounced than that of dry b_{sp}. Higher values (36.8 Mm^{-1}) of the absorption coefficient appeared at 8:00 LST, mainly attributed to the severe emission of light-absorbing pollutants during the morning traffic rush hours. Both the mean and median values were enhanced at night, with a maximum hourly mean value of 35.5 Mm^{-1} (19:00 LST). The mean and median values then fell between 19:00 and 08:00 the next day, with a minimum hourly mean value of 18.8 Mm^{-1} at 02:00 LST. As seen in Fig. 7c, the diurnal cycle observed for SSA is a mirror image of the b_{ap} cycle. The maximum hourly mean values (0.90–0.91) occurred during the daytime (10:00–14:00) and the minimum hourly mean values (0.87–0.88) occurred in the morning (07:00–08:00). The curve shape of the SSA is analogous to that measured at Beijing (Han et al., 2014c) and Guangzhou (Garland et al., 2008). That is, the shape of the SSA curve from sunrise to sunset is an arc, which should relate to the photochemical reactions and new particle formation in the air. This phenomenon is worthy of further study.

2.3. Characteristics of aerosol optical properties and their interrelationship with chemical compositions

Fig. 8a, b illustrates the relationship between b_{sp}, b_{ap} and the mass concentration of $PM_{2.5}$ in Shanghai during the whole

Table 3 – Statistical summary of mean f(RH) values for $(NH_4)_2SO_4$ and NH_4NO_3 in selected relative humidity ranges.

RH (%)	20–25	25–30	30–35	35–40	40–45	45–50	50–55	55–60	60–65	65–70	70–75	75–80	80–85	85–90	>90
f(RH)	1.06	1.11	1.16	1.21	1.22	1.27	1.33	1.38	1.45	1.55	1.65	1.83	2.10	2.46	3.17

jesc.ac.cn

Table 4 – Composite variables for particulate matter proposed by IMPROVE.

Component	Specification	Mass calculation
$(NH_4)_2SO_4$	Ammonium sulfate	$0.944[NH_4^+] + 1.02[SO_4^{2-}]$ [a]
NH_4NO_3	Ammonium nitrate	$1.29[NO_3^-]$
OMC	Organic mass by carbon	1.6[OC] [b]
b_{abs}	Absorption coefficient	[EC]
CM	Coarse mass	$[PM_{10}] - [PM_{2.5}]$

[a] Malm and Day, 2001; Tao et al., 2009.
[b] Turpin and Lim, 2001.

campaign, respectively. In Fig. 8a, b_{sp} showed a strong and positive correlation with $PM_{2.5}$ mass concentration with a correlation coefficient of 0.98. As shown in Fig. 8b, b_{ap} was also strongly correlated ($r = 0.93$) with $PM_{2.5}$ mass concentration. MSE is aerosol mass scattering efficiency, and MAE is aerosol mass absorption efficiency, being the ratio of the measured aerosol scattering coefficient and absorption coefficient to the mass concentration of particulate matter, respectively. In this study, the slopes of the regression lines can be regarded as the average mass scattering/absorption efficiency. It could be concluded from Fig. 8a and b that the mean values for MSE and MAE were 5.6 and 0.5 m^2/g, respectively. The value of MSE was 3.2 m^2/g and MAE 0.8 m^2/g in Guangzhou during the 2006 PRIDE-PRD campaign (Liu et al., 2012). Liu et al. (2013a) determined that the MSE and MAE for $PM_{2.5}$ were 3.97 and 0.62 m^2/g in Beijing from October 24 to November 9, 2007.

Extinction by fine soil could be neglected from the standpoint of light extinction in summer (Liu et al., 2009; Han et al., 2014c). Thus, the modified IMPROVE algorithm is presented as Eq. (9).

$$b_{ext} \approx 3f(RH) \times [(NH_4)_2SO_4] + 3f(RH) \times [NH_4NO_3] + 4 \times [POM] + 10 \times [EC] + 0.6 \times [CoarseMass] + 10 \quad (9)$$

Table 3 summarizes different f(RH) values for $(NH_4)_2SO_4$ and NH_4NO_3 in selected relative humidity ranges (Malm and Day, 2001; Liu et al., 2012; Han et al., 2014c). Table 4 lists the composite variables for particulate matter proposed by IMPROVE. According to Eqs. (3), (4), (5), (7) and (9), the calculated b_{ext} can be derived.

Fig. 9 signifies the averaged mass proportion of chemical components in $PM_{2.5}$ during the campaign for non-haze and haze days. Ammonium sulfate, ammonium nitrate, organic mass and elemental carbon accounted for 23.7%, 21.5%, 22.4% and 4.5% of the mass concentration of $PM_{2.5}$ during non-haze days; the corresponding values were 32.5%, 21.9%, 21% and 4.4% during hazy days. Ammonium sulfate, ammonium nitrate and POM accounted for 20.2%, 11.2% and 15.8% of the mass concentration of PM_{10} during clean days, and 34.0%, 19.1% and 13.9% during hazy days in Beijing (Han et al., 2014c);

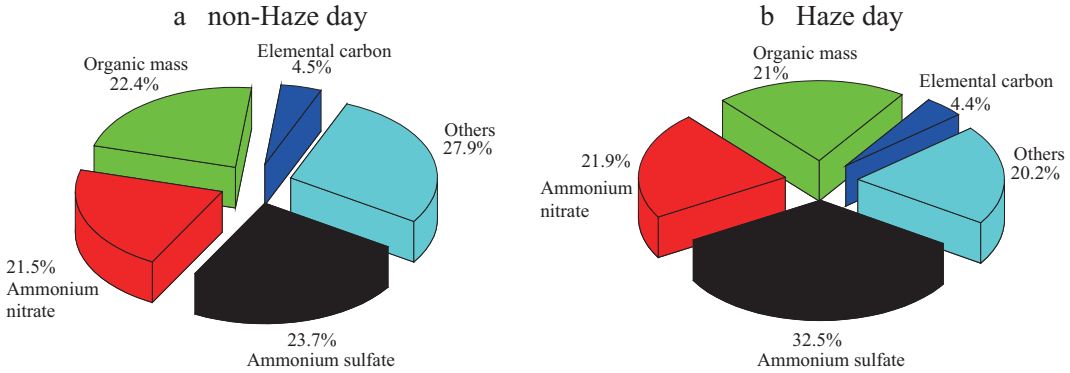

Fig. 9 – The averaged mass proportion of the chemical components in $PM_{2.5}$ under (a) non-haze days, and (b) haze days in Shanghai.

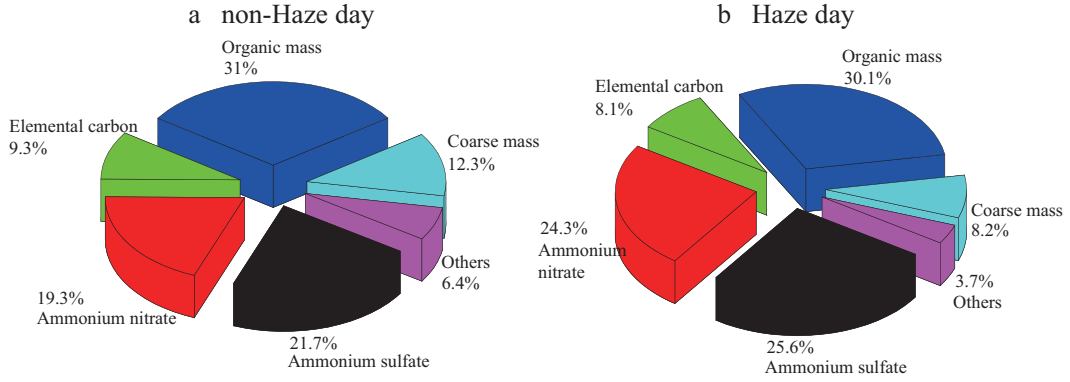

Fig. 10 – Averaged fractional contributions to extinction coefficient by chemical components under (a) non-haze days, and (b) haze days in Shanghai.

jesc.ac.cn

while as depicted in Fig. 10, ammonium sulfate, ammonium nitrate, organic mass, elemental carbon and coarse mass accounted for 21.7%, 19.3%, 31.0%, 9.3% and 12.3% of the total extinction coefficient during non-haze days, and 25.6%, 24.3%, 30.1%, 8.1% and 8.2% during hazy days. As shown in Fig. 10, organic mass was the largest contributor to b_{ext}, which was comparable to the value of Xiamen (39.5%) (Zhang et al., 2012). The results implied that organic mass was the largest contributor to visibility degradation in Shanghai. However, ammonium sulfate was the largest contributor to visibility degradation in Hong Kong (Cheung et al., 2005), Jinan (Yang et al., 2007), Beijing (Han et al., 2014c) and Guangzhou (Tao et al., 2009) in China and in the eastern United States (Watson, 2002). Meanwhile, the contribution proportions of ammonium sulfate and ammonium nitrate to light extinction were significantly higher during the hazy time than during the non-haze days, while the contribution proportions of organic mass, elemental carbon and coarse mass to b_{ext} were lower during the hazy time than during the non-haze days.

3. Conclusions

A field campaign was carried out from December 1 to 31, 2012, wherein aerosol optical and physical properties as well as aerosol chemical components were measured simultaneously. In this study, we analyzed the characteristics of the aerosol optical properties and explored their relationships to the changes in chemical components.

The hazy time accounted for 11.4% of the whole campaign. The concentrations of the air pollutants NO_2, NOx, NO, SO_2, CO, and $PM_{2.5}$ had an increasing trend during the haze episodes. The mass loading of $PM_{2.5}$ gradually accumulated, and its instantaneous value reached 173.8 $\mu g/m^3$. The average values of SO_4^{2-}, NO_3^- and NH_4^+ during the haze episodes all exceeded the average values of these components during the non-haze days. The atmospheric aerosol scattering coefficient b_{sp}, aerosol absorption coefficient b_{ap}, and single scattering albedo ω at 550 nm during the whole campaign were 288.7 (186.3), 27.7 (17.6) and 0.91 (0.04)Mm^{-1}, respectively.

A bi-peak distribution was observed for the mass concentrations of CO, NO_2, NOx and NO. Because of the more active photochemistry, more sulfate was produced during daytime than in the evening. The mass concentration of ammonium achieved a small peak at 12:00 LST. The time when it reached the second peak was 17:00 LST. The diurnal variations of nitrate showed little hourly variation, with lower concentrations in the afternoon and higher concentrations in the early morning. There were obvious bi-peak diurnal patterns for b_{sp}, b_{ap} as well as SSA. The diurnal cycle for b_{ap} was even more pronounced than that of dry b_{sp}. Higher values of the b_{ap} appeared at 8:00 LST. The diurnal cycle observed for SSA is a mirror image of the b_{ap} cycle.

b_{sp} and b_{ap} showed strong and positive correlations with $PM_{2.5}$ mass concentration. Ammonium sulfate, ammonium nitrate, organic mass, elemental carbon and coarse mass accounted for 21.7%, 19.3%, 31.0%, 9.3% and 12.3% of the total extinction coefficient during non-haze days, and 25.6%, 24.3%, 30.1%, 8.1% and 8.2% during hazy days. Organic mass was the largest contributor to b_{ext} in Shanghai. The contribution proportions of ammonium sulfate and ammonium nitrate to b_{ext} were significantly higher during the hazy time than during the non-haze days, while the contribution proportions of organic mass, elemental carbon and coarse mass to b_{ext} were contrary.

Acknowledgments

This work was supported by the Ministry of Science and Technology of China (No. 2013CB955804), the National Natural Science Foundation of China (Nos. 41175018, 41475113), and the Ministry of Environmental Protection of China (Nos. 201209001, 201409008, 201209007).

REFERENCES

Alados-Arboledas, L., Alcántara, A., Olmo, F.J., Martínez-Lozano, J.A., Estellés, V., Cachorro, V., et al., 2008. Aerosol columnar properties retrieved from CIMEL radiometers during VELETA 2002. Atmos. Environ. 42, 2654–2667.

Andreae, M.O., Schmid, O., Yang, H., Chand, D., Yu, J.Z., Zeng, L.M., et al., 2008. Optical properties and chemical composition of the atmospheric aerosol in urban Guangzhou China. Atmos. Environ. 42, 6335–6350.

Bergin, M.H., Cass, G.R., Xu, J., Fang, C., Zeng, L.M., Yu, T., et al., 2001. Aerosol radiative, physical, and chemical properties in Beijing during June 1999. J. Geophys. Res. 106, 17969–17980.

Bokoye, A.I., Royer, A., O'Neill, N.T., Fedosejevs, G., Teillet, P.M., McArthur, B., 2001. Characterization of atmospheric aerosols across Canada. Assessment from a ground-based Sunphotometer network: AEROCAN. Atmo. Ocean 39 (4), 429–456.

Campanelli, M., Estellés, V., Tomasi, C., Nakajima, T., Malvestuto, V., Martínez-Lozano, J.A., 2007. Application of the SKYRAD improved Langley plot method for the in situ calibration of CIMEL Sun-sky photometers. Appl. Opt. 46, 2688–2702.

Cao, J.J., Wang, Q.Y., Chow, J.C., Watson, J.G., Tie, X.X., Shen, Z.X., et al., 2012. Impacts of aerosol compositions on visibility impairment in Xi'an, China. Atmosph. Environ. 59, 559–566.

Chan, C.K., Yao, X., 2008. Air pollution in megacities in China. Atmosph. Environ. 42, 1–42.

Chan, Y.C., Simpson, R.W., Mctainsh, G.H., Vowles, P.D., Cohen, D.D., Bailey, G.M., 1999. Source apportionment of visibility degradation problems in Brisbane (Australia) using the multiple linear regression techniques. Atmos. Environ. 33, 3237–3325.

Cheung, H.C., Wang, T., Baumann, K., Guo, H., 2005. Influence of regional pollution outflow on the concentrations of fine particulate matter and visibility in the coastal area of southern China. Atmos. Environ. 39, 6463–6474.

Chýlek, P., Wong, J., 1995. Effect of absorbing aerosols on global radiation budget. Geophys. Res. Lett. 22 (8), 929–931.

Du, H.H., Kong, L.D., Cheng, T.T., Chen, J.M., Du, J.F., Li, L., et al., 2011. Insights into summertime haze pollution events over Shanghai based on online water-soluble ionic composition of aerosols. Atmos. Environ. 45, 5131–5137.

Eidels-Dubovoi, S., 2002. Aerosol impacts on visible light extinction in the atmosphere of Mexico City. Sci. Total Environ. 287, 213–220.

Formenti, P., Boucher, O., Reiner, T., Sprung, D., Andreae, M.O., 2002. STARTE-MED 1998 summer airborne measurements over the Aegean Sea 2. Aerosol scattering and absorption, and radiative calculations. J. Geophys. Res. 107. http://dx.doi.org/10.1029/2001JD001536.

jesc.ac.cn

Garland, R.M., Yang, H., Schmid, O., Rose, D., Nowak, A., Achtert, P., et al., 2008. Aerosol optical properties in a rural environment near the mega-city Guangzhou, China: implications for regional air pollution, radiative forcing and remote sensing. Atmos. Chem. Phys. 8, 5161–5186.

Goloub, P., Li, Z., Dubovik, O., Blarel, L., Podvin, T., Jankowiak, I., et al., 2008. PHOTONS/AERONET sunphotometer network overview: description, activities, results. Fourteenth international symposium on atmospheric and ocean optics/atmospheric physics. Proc. SPIE 69360.

Han, T.T., Liu, X.G., Zhang, Y.H., Gu, J.W., Tian, H.Z., Zeng, L.M., et al., 2014a. Chemical characteristics of PM_{10} during the summer in the mega-city Guangzhou. China. Atmos. Res. 137, 25–34.

Han, T.T., Liu, X.G., Zhang, Y.H., Qu, Y., Gu, J.W., Ma, Q., et al., 2014b. Characteristics of aerosol optical properties and their chemical apportionments during CAREBeijing 2006. Aerosol Air Qua. Res. http://dx.doi.org/10.4209/aaqr.2013.06.0203.

Han, T.T., Liu, X.G., Zhang, Y.H., Qu, Y., Ma, Q., Tian, H.Z., Zeng, L.M., Hu, M., Zhu, T., 2014c. Role of secondary aerosols on haze formation in summer in the megacity Beijing. J. Environ. Sci, China (accepted for publication).

Holben, B.N., Eck, T.F., Slutsker, I., Tanre, D., Buis, J.P., Setzer, A., et al., 1998. AERONET—A federated instrument network and data archive for aerosol characterization. Remote Sens. Environ. 66, 1–16.

Huang, X.F., He, L.Y., Xue, L., Sun, T.L., Zeng, L.W., Gong, Z.H., et al., 2012a. Highly time-resolved chemical characterization of atmospheric fine particles during 2010 Shanghai World Expo. Atmos. Chem. Phys. 12, 4897–4907.

Huang, K., Zhuang, G., Lin, Y., Fu, J.S., Wang, Q., Liu, T., et al., 2012b. Typical types and formation mechanisms of haze in an Eastern Asia megacity, Shanghai. Atmos. Chemi. Phys. 12, 105–124. http://dx.doi.org/10.5194/acp-12-105-2012.

Jung, J., Lee, H., Kim, Y.J., Liu, X., Zhang, Y., Hu, M., et al., 2009. Optical properties of atmospheric aerosols obtained by in situ and remote measurements during 2006 Campaign of Air Quality Research in Beijing (CAREBeijing—2006). J. Geophys. Res. 114 http://dx.doi.org/10.1029/2008JD010337.

Kim, D.H., Sohn, B.J., Nakajima, T., Takamura, T., Choi, B.C., Yoon, S.C., 2004. Aerosol optical properties over East Asia determined from ground-based sky radiation measurements. J. Geophys. Res. 109. http://dx.doi.org/10.1029/2003JD003387.

Li, C., Marufu, L.T., Dickerson, R.R., Li, Z.T., Wen, Y., Wang, P., et al., 2007. In situ measurements of trace gases and aerosol optical properties at a rural site in northern China during East Asian Study of Tropospheric Aerosols: an International Regional Experiment 2005. J. Geophys. Res. 112 http://dx.doi.org/10.1029/2006JD007592.

Liu, X.G., Cheng, Y.F., Zhang, Y.H., Jung, J.S., Sugimoto, N., Chang, S.Y., et al., 2008. Influences of relative humidity and particle chemical composition on aerosol scattering properties during the 2006 PRD campaign. Atmos. Environ. 42, 1525–1536.

Liu, X.G., Zhang, Y.H., Jung, J.S., Gu, J.W., Li, Y.P., Guo, S., et al., 2009. Research on aerosol hygroscopic properties by measurement and model during the 2006 CARE Beijing campaign. J. Geophys. Res. 114. http://dx.doi.org/10.1029/2008JD010805.

Liu, X.G., Zhang, Y.H., Cheng, Y.F., Hu, M., Han, T.T., 2012. Aerosol hygroscopicity and its impact on atmospheric visibility and radiative forcing in Guangzhou during the 2006 PRIDE-PRD campaign. Atmos. Environ. 60, 59–67.

Liu, X.G., Gu, J.W., Li, Y.P., Cheng, Y.F., Qu, Y., Han, T.T., et al., 2013a. Increase of aerosol scattering by hygroscopic growth: observation, modeling, and implications on atmospheric visibility. Atmos. Res. 132–133, 91–101.

Liu, X.G., Li, J., Qu, Y., Han, T.T., Hou, L., Gu, J.W., et al., 2013b. Formation and evolution mechanism of regional haze: a case study in mega-city Beijing of China. Atmos. Chem. Phys. 13, 4501–4514.

Lyamani, H., Olmoa, F.J., Alados-Arboledas, L., 2008. Light scattering and absorption properties of aerosol particles in the urban environment of Granada, Spain. Atmos. Environ. 42, 2630–2642.

Malm, W.C., Day, D.E., 2001. Estimates of aerosol species scattering characteristics as a function of relative humidity. Atmos. Environ. 35, 2845–2860.

Malm, W.C., Hand, J.L., 2007. An examination of the physical and optical properties of aerosols collected in the IMPROVE program. Atmos. Environ. 41, 3407–3427.

O'Brien, D.M., Mitchell, R.M., 2003. Atmospheric heating due to carbonaceous aerosol in northern Australia—confidence limits based on TOMS aerosol index and sun-photometer data. Atmos. Res. 66, 21–41.

Seinfeld, J.H., Pandis, S.N., 2006. Atmospheric Chemistry and Physics: From Air Pollution to Climate Change, 2nd ed. John Wiley & Sons Inc., New York, USA.

Tao, J., Ho, K.F., Chen, L.G., Zhu, L.H., Han, J.L., Xu, Z.C., 2009. Effect of chemical composition of $PM_{2.5}$ on visibility in Guangzhou, China, 2007 spring. Particuology 7, 68–75.

Turpin, B.J., Lim, H.J., 2001. Species contributions to $PM_{2.5}$ mass concentrations: revisiting common assumptions for estimating organic mass. Aerosol Sci. Technol. 35, 602–610.

Uchiyama, A., Yamazaki, A., Togawa, H., Asano, J., 2005. Characteristics of aeolian dust observed by sky-radiometer in the Intensive Observation Period 1 (IOP1). J. Meteorol. Soc. Jpn 83A, 291–305.

Wang, S.X., Hao, J.M., 2012. Air quality management in China: issues, challenges, and options. J. Environ. Sci. 24, 2–13.

Wang, K.C., Dickinson, R.E., Liang, S.L., 2009. Clear sky visibility has decreased over land globally from 1973 to 2007. Science 323, 1468–1470.

Wang, X.M., Ding, X., Fu, X.X., He, Q.F., Wang, S.Y., Bernard, F., et al., 2012. Aerosol scattering coefficients and major chemical compositions of fine particles observed at a rural site hit the central Pearl River Delta, South China. J. Environ. Sci. 24, 72–77.

Watson, J.G., 2002. Visibility: science and regulation. J. Air Waste Manage. Assoc. 52, 628–713.

Wu, D., Bi, X., Deng, X., Li, F., Tan, H., Liao, G., et al., 2006. Effects of atmospheric haze on the deterioration of visibility over the Pearl River Delta. Acta Meteor. Sinica. 64, 510–517.

Xu, J., Bergin, M.H., Yu, X., Liu, G., Zhao, J., Carrico, C.M., et al., 2002. Measurement of aerosol chemical, physical and radiative properties in the Yangtze delta region of China. Atmos. Environ. 36, 161–173.

Xu, J.W., Tao, J., Zhang, R.J., Cheng, T.T., Leng, C.P., Chen, J.M., et al., 2012. Measurements of surface aerosol optical properties in winter of Shanghai. Atmos. Res. 109–110, 25–35.

Yang, L.X., Wang, D.C., Cheng, S.H., Wang, Z., Zhou, Y., Zhou, X.H., et al., 2007. Influence of meteorological conditions and particulate matter on visual range impairment in Jinan, China. Sci. Total Environ. 383, 164–173.

Zhang, F.W., Xu, L.L., Chen, J.S., Yu, Y.K., Niu, Z.C., Yin, L.Q., 2012. Chemical compositions and extinction coefficients of $PM_{2.5}$ in peri-urban of Xiamen, China, during June 2009–May 2010. Atmos. Res. 106, 150–158.

jesc.ac.cn

Editorial Board of Journal of Environmental Sciences

Editor-in-Chief

X. Chris Le University of Alberta, Canada

Associate Editors-in-Chief

Jiuhui Qu Research Center for Eco-Environmental Sciences, Chinese Academy of Sciences, China
Shu Tao Peking University, China
Nigel Bell Imperial College London, UK
Po-Keung Wong The Chinese University of Hong Kong, Hong Kong, China

Editorial Board

Aquatic environment

Baoyu Gao
Shandong University, China
Maohong Fan
University of Wyoming, USA
Chihpin Huang
National Chiao Tung University
Taiwan, China
Ng Wun Jern
Nanyang Environment &
Water Research Institute, Singapore
Clark C. K. Liu
University of Hawaii at Manoa, USA
Hokyong Shon
University of Technology, Sydney, Australia
Zijian Wang
Research Center for Eco-Environmental Sciences,
Chinese Academy of Sciences, China
Zhiwu Wang
The Ohio State University, USA
Yuxiang Wang
Queen's University, Canada
Min Yang
Research Center for Eco-Environmental Sciences,
Chinese Academy of Sciences, China
Zhifeng Yang
Beijing Normal University, China
Han-Qing Yu
University of Science & Technology of China,
China

Terrestrial environment

Christopher Anderson
Massey University, New Zealand
Zucong Cai
Nanjing Normal University, China
Xinbin Feng
Institute of Geochemistry,
Chinese Academy of Sciences, China
Hongqing Hu
Huazhong Agricultural University, China
Kin-Che Lam
The Chinese University of Hong Kong
Hong Kong, China
Erwin Klumpp
Research Centre Juelich, Agrosphere Institute
Germany
Peijun Li
Institute of Applied Ecology,
Chinese Academy of Sciences, China
Michael Schloter
German Research Center for Environmental Health
Germany
Xuejun Wang
Peking University, China
Lizhong Zhu
Zhejiang University, China

Atmospheric environment

Jianmin Chen
Fudan University, China
Abdelwahid Mellouki
Centre National de la Recherche Scientifique
France
Yujing Mu
Research Center for Eco-Environmental Sciences,
Chinese Academy of Sciences, China
Min Shao
Peking University, China
James Jay Schauer
University of Wisconsin-Madison, USA
Yuesi Wang
Institute of Atmospheric Physics,
Chinese Academy of Sciences, China
Xin Yang
University of Cambridge, UK

Environmental biology

Yong Cai
Florida International University, USA
Henner Hollert
RWTH Aachen University, Germany
Jae-Seong Lee
Sungkyunkwan University, South Korea
Christopher Rensing
University of Copenhagen, Denmark
Bojan Sedmak
National Institute of Biology, Slovenia
Lirong Song
Institute of Hydrobiology,
Chinese Academy of Sciences, China
Chunxia Wang
National Natural Science Foundation of China
Gehong Wei
Northwest A & F University, China
Daqiang Yin
Tongji University, China
Zhongtang Yu
The Ohio State University, USA

Environmental toxicology and health

Jingwen Chen
Dalian University of Technology, China
Jianying Hu
Peking University, China
Guibin Jiang
Research Center for Eco-Environmental Sciences,
Chinese Academy of Sciences, China
Sijin Liu
Research Center for Eco-Environmental Sciences,
Chinese Academy of Sciences, China
Tsuyoshi Nakanishi
Gifu Pharmaceutical University, Japan
Willie Peijnenburg
University of Leiden, The Netherlands
Bingsheng Zhou
Institute of Hydrobiology,
Chinese Academy of Sciences, China

Environmental catalysis and materials

Hong He
Research Center for Eco-Environmental Sciences,
Chinese Academy of Sciences, China
Junhua Li
Tsinghua University, China
Wenfeng Shangguan
Shanghai Jiao Tong University, China
Ralph T. Yang
University of Michigan, USA

Environmental analysis and method

Zongwei Cai
Hong Kong Baptist University,
Hong Kong, China
Jiping Chen
Dalian Institute of Chemical Physics,
Chinese Academy of Sciences, China
Minghui Zheng
Research Center for Eco-Environmental Sciences,
Chinese Academy of Sciences, China

Municipal solid waste and green chemistry

Pinjing He
Tongji University, China

Editorial office staff

Managing editor Qingcai Feng
Editors Zixuan Wang Suqin Liu Kuo Liu Zhengang Mao
English editor Catherine Rice (USA)

Copyright© Research Center for Eco-Environmental Sciences, Chinese Academy of Sciences. Published by Elsevier B.V. and Science Press. All rights reserved.

JOURNAL OF ENVIRONMENTAL SCIENCES

环境科学学报(英文版)

www.jesc.ac.cn

Aims and scope

Journal of Environmental Sciences is an international academic journal supervised by Research Center for Eco-Environmental Sciences, Chinese Academy of Sciences. The journal publishes original, peer-reviewed innovative research and valuable findings in environmental sciences. The types of articles published are research article, critical review, rapid communications, and special issues.

The scope of the journal embraces the treatment processes for natural groundwater, municipal, agricultural and industrial water and wastewaters; physical and chemical methods for limitation of pollutants emission into the atmospheric environment; chemical and biological and phytoremediation of contaminated soil; fate and transport of pollutants in environments; toxicological effects of terrorist chemical release on the natural environment and human health; development of environmental catalysts and materials.

For subscription to electronic edition

Elsevier is responsible for subscription of the journal. Please subscribe to the journal via http://www.elsevier.com/locate/jes.

For subscription to print edition

China: Please contact the customer service, Science Press, 16 Donghuangchenggen North Street, Beijing 100717, China. Tel: +86-10-64017032; E-mail: journal@mail.sciencep.com, or the local post office throughout China (domestic postcode: 2-580).

Outside China: Please order the journal from the Elsevier Customer Service Department at the Regional Sales Office nearest you.

Submission declaration

Submission of the work described has not been published previously (except in the form of an abstract or as part of a published lecture or academic thesis), that it is not under consideration for publication elsewhere. The publication should be approved by all authors and tacitly or explicitly by the responsible authorities where the work was carried out. If the manuscript accepted, it will not be published elsewhere in the same form, in English or in any other language, including electronically without the written consent of the copyright-holder.

Editorial

Authors should submit manuscript online at http://www.jesc.ac.cn. In case of queries, please contact editorial office, Tel: +86-10-62920553, E-mail: jesc@rcees.ac.cn. Instruction to authors is available at http://www.jesc.ac.cn.

Journal of Environmental Sciences (Established in 1989)
Volume 27 2015

Supervised by	Chinese Academy of Sciences	**Published by**	Science Press, Beijing, China
Sponsored by	Research Center for Eco-Environmental		Elsevier Limited, The Netherlands
	Sciences, Chinese Academy of Sciences	**Distributed by**	
Edited by	Editorial Office of Journal of	Domestic	Science Press, 16 Donghuangchenggen
	Environmental Sciences		North Street, Beijing 100717, China
	P. O. Box 2871, Beijing 100085, China		Local Post Offices through China
	Tel: 86-10-62920553; http://www.jesc.ac.cn	Foreign	Elsevier Limited
	E-mail: jesc@rcees.ac.cn		http://www.elsevier.com/locate/jes
Editor-in-chief	X. Chris Le	**Printed by**	Beijing Beilin Printing House, 100083, China

CN 11-2629/X **Domestic postcode: 2-580** **Domestic price per issue RMB ¥ 110.00**

ISSN 1001-0742